

## Cold atomic beam produced by a conical mirror funnel

K. H. Kim, K. I. Lee, H. R. Noh, and W. Jhe\*

*Center for Near-field Atom-photon Technology and Physics Department, Seoul National University, Seoul 151-742, Korea*

N. Kwon

*Physics Department, Hankuk University of Foreign Studies, Yongin 449-791, Korea*

M. Ohtsu

*Interdisciplinary Graduate School, Tokyo Institute of Technology, Yokohama 226, Japan*

(Received 17 November 2000; published 31 May 2001)

We have obtained and characterized a cold atomic beam produced by a simple conical atom funnel, which consists of a conical hollow mirror (axicon) with a small hole at the apex and a single incident laser beam. Atoms trapped in the axicon mirror are ejected by the radiation-pressure imbalance along the extraction column. The atomic beam has a longitudinal velocity in the range of 4 to 6 m/s, a divergence of 150 mrad, and a maximum instantaneous flux of  $2.2 \times 10^{10}$  atoms/s in a pulsed operation. The experimental results are in quantitative agreement with the numerical simulations. A continuous atomic beam is also possible with an apex hole smaller than the trapped atomic cloud.

DOI: 10.1103/PhysRevA.64.013402

PACS number(s): 32.80.Pj

A cold atomic beam (CAB) has been used in many applications of precision spectroscopy and atom optics experiments [1] such as atom interferometer, atom lithography, and atomic clock. In particular, Bose-Einstein condensation [2] requires an efficient way to transfer cold atoms from a high-pressure magneto-optical trap (MOT) to a high-vacuum region providing a long trap lifetime. Several methods to produce CAB's have been developed: Zeeman-tuned slowing [3], chirped cooling [4], slowing by broadband laser [5], and slowing by isotropic light [6]. Recently, another method that uses trapped atoms was demonstrated. Lu *et al.* [7] produced a low-velocity intense source of atoms with a continuous flux of  $5 \times 10^9$  atoms/s extracted from a standard vapor-cell MOT. A simpler way of producing a continuous source of cold atoms was also demonstrated [8,9] by use of a single-beam pyramidal mirror MOT [10].

In this paper, we report on the compact and simple production of slow and intense CAB's [11] by using a simple single-beam conical mirror MOT [12] that has a small hole at the apex. Compared to the pyramidal system, that is basically equivalent to the typical six-beam MOT system [7], the axicon scheme has several interesting features such as the cylindrical symmetry and the focusing effect of the axicon mirror. Moreover, due to its simplicity and available low atomic velocity, there is much increasing interest in many-atom optical applications. In particular, the simple CAB system may be useful for loading high-vacuum MOT [9] and the microscopic atom-optical elements [13]. On the other hand, there has been not much quantitative study of the properties of the CAB in the axicon with respect to the laser intensity or the detuning. In this work, we study in detail CAB characteristics, such as velocity distribution and the collimation effect, which are all in good agreement with the numerical simulations.

The conical funnel that produces the CAB consists of a conical hollow mirror having a 2-cm entrance diameter and a 2-mm hole at the apex. When a single laser beam with a given circular polarization is incident along the axicon axis, first reflections at the conical surface generate infinite radial pairs of counterpropagating transverse lights with opposite polarizations. Moreover, except near the on-axis region (i.e., the extraction column), where there is a small hole, a laser beam, with polarization and propagation directions opposite to those of the incident laser, is also generated as a result of two reflections of the single incident laser at the axicon surface. In order to trap cold atoms near the mirror axis inside the hollow region, one needs to send an additional counterpropagating laser light along the extraction column through the axicon-apex hole, which has the same detuning and intensity with respect to those of the incident laser light. Note that one can easily adjust the MOT position inside the hollow region by moving the magnetic-field null point of the anti-Helmholtz coils, which is the basic working principle for a MOT near a microstructure on a surface (the so-called surface MOT) [13]. To obtain the CAB, one may first move the MOT toward the mirror axis and then switch off the additional counter propagating laser beam and the magnetic field. Atoms are then pushed toward the apex, and are extracted from the conical funnel due to the imbalanced radiation pressure along the extraction column.

The experimental setup is shown in Fig. 1(a). For cooling and trapping of  $^{85}\text{Rb}$ , we have used an external-cavity diode-laser that is  $-2.5\Gamma$  detuned from the  $5S_{1/2, F=3} \rightarrow 5P_{3/2, F'=4}$  transition of  $^{85}\text{Rb}$ , where  $\Gamma$  ( $=2\pi \times 5.9$  MHz) is the spontaneous decay rate of the excited state. For repumping, we use the  $5S_{1/2, F=2} \rightarrow 5P_{3/2, F'=3}$  absorption line. An acousto-optic modulator (AOM1) is used for a fast change of the intensity of the incident trapping laser, which also works as a pushing laser when the counter-propagating beam is blocked. The trapping beam is first sent

\*Email address: whjhe@snu.ac.kr

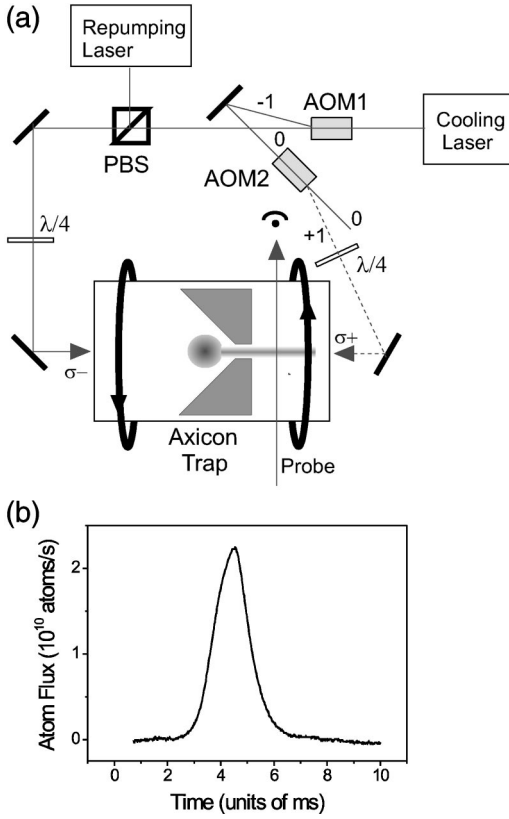


FIG. 1. (a) Schematic of the conical mirror funnel used to produce a cold atomic beam. When the counterpropagating beam with respect to the incident laser is switched off, the trapped atoms are pushed out of the axicon mirror through the 2-mm hole at the apex by the imbalanced radiation pressure along the extraction column. Here the incident cooling and trapping laser beam serves as a pushing laser. AOM1 is used for rapid change of the pushing-laser intensity, whereas AOM2 is for switching the counterpropagating beam on and off. (b) A typical absorption signal of the pulsed atomic beam detected by the probe laser in the downstream. The mean longitudinal velocity is about 4.2 m/s.

to AOM1, and then splits into two beams: the zeroth-order beam is combined with the repumping light by a polarizing beam splitter, and then sent to the axicon after being circularly polarized. On the other hand, the first-order diffracted beam, which is  $-80$  MHz frequency shifted, is further diffracted and frequency shifted by  $+80$  MHz by another acousto-optic modulator (AOM2). This beam is then sent along the opposite direction with respect to the incident laser through the axicon hole, to provide a counterpropagating laser beam that is necessary for the MOT. Therefore, this additional laser beam can be switched on and off by AOM2. A quadrupole magnetic field for the MOT is generated by a pair of anti-Helmholtz coils that are oriented along the axicon axis outside the glass vacuum cell (the pressure inside is less than  $10^{-8}$  Torr), and mounted on the  $xyz$  translator, so that the MOT position can be conveniently adjusted along the extraction column.

To characterize the produced CAB, we place a probe laser whose frequency is tuned to the transition  $5S_{1/2, F=3} \rightarrow 5P_{3/2, F'=4}$ . The probe beam is 1 mm wide and 10 mm

high, and is placed 10 mm downstream from the axicon apex, crossing the atoms at a right angle. We have detected the probe absorption due to the extracted CAB by using a photodiode. This allows one to measure the flux, the spatial distribution, and the velocity distribution of the CAB. The laser power absorbed by the atoms inside the probe laser is given by

$$\Delta P_{abs} = f \frac{\Gamma}{2} \frac{I}{I + I_s} \hbar \omega \frac{\Delta x}{v_z}, \quad (1)$$

where  $f$  is the atomic flux (atoms/s),  $v_z$  is the longitudinal atomic velocity,  $\Delta x$  is the width of the probe laser,  $I$  is the probe-laser intensity, and  $I_s = 3.78$  mW/cm<sup>2</sup> is the saturation intensity averaged over the magnetic sublevels of the <sup>85</sup>Rb ground state. Note that one can estimate the atomic flux  $f$  from Eq. (1).

A typical absorption signal of the CAB is shown in Fig. 1(b), where the incident-laser intensity is 0.5 mW/cm<sup>2</sup> and the detuning is  $-2.5\Gamma$ . Note that we obtain a pulsed CAB since the apex hole is larger than the MOT size. Of course, when the MOT is made larger than the hole diameter, one can obtain a continuous CAB [14]. The arrival time of the CAB determines the longitudinal velocity, whereas the width is associated with its velocity spread. The average velocity and the full width at half maximum obtained from the absorption signal in Fig. 1(b) are 4.2 and 0.54 m/s, respectively. From the numerical simulation, we have found that the velocity width depends mostly on the size of the MOT. This is due to the fact that the trap size is not negligible compared to the separation between the MOT and the probe laser (the measured  $e^{-1/2}$  radius of the MOT is about 1 mm, whereas the MOT-apex separation is about 3–4 mm). Under various experimental conditions of different intensities and detunings of the laser, the longitudinal atomic velocity varies from 4 to 6 m/s.

From Eq. (1), we have obtained a maximum flux of  $2.2 \times 10^{10}$  atoms/s per pulse, which is mainly determined by the number of the trapped atoms in the MOT. For the CAB experiment in Ref. [7], a continuous flux of  $5 \times 10^9$  atoms/s and a pulsed flux that is ten times larger were obtained. Even though we have used low-power diode lasers in contrast to the high-power Ti:sapphire laser used in Ref. [7], we are able to obtain a comparable atomic beam flux. This may be attributed to the fact that a higher laser intensity is available near the axicon axis due to its focusing effect [15]. Note that, by using a larger conical funnel and a higher laser power, one can obtain a higher-flux CAB [14]. Compact and easy construction and convenient control are the major advantages of our simple CAB system using the axicon-mirror atom funnel.

We have measured the number of extracted atoms versus the pushing-beam intensity, and the results are presented in Fig. 2. Figure 2(a) shows the total number of atoms in the CAB versus the pushing-beam intensity at a detuning of  $-2.5\Gamma$ . The experimental data show that the flux is maximum near a laser intensity of 0.5 mW/cm<sup>2</sup>, whereas it decreases beyond 0.7 mW/cm<sup>2</sup>, which is in good agreement with the numerical simulation. By contrast, in Ref. [7] the

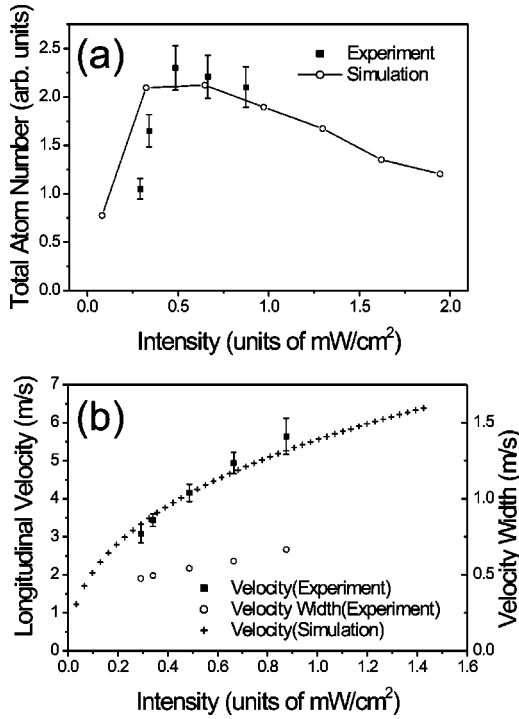


FIG. 2. (a) Experimental and simulational results for the total number of atoms extracted from the axicon funnel vs the pushing-beam intensity at a given detuning of  $-2.5\Gamma$ . (b) The mean value and the width of the atomic velocity distribution.

maximum flux was obtained at about  $40 \text{ mW/cm}^2$ . This may be associated with the focusing effect of the incident light toward the mirror axis inside the axicon. Since the intensity increases in approximate proportion to  $1/r$ , where  $r$  is the radial distance from the axicon axis, one has to consider the atomic motion in the nonuniform-intensity counterpropagating beams [15].

Let us consider the simple case of one-dimensional motion in the transverse plane of the axicon. At low velocities such that  $k_L v \ll \Gamma$ , the scattering force experienced by the atoms due to the  $F=0 \rightarrow F'=1$  transition in the counter-propagating  $\sigma^+ - \sigma^-$  laser beams is given by  $F_T = -\alpha v_r$ , where the damping coefficient  $\alpha$  is given by Ref. [16]:

$$\alpha = -\hbar k_L^2 \frac{2s}{1+2s} \frac{4\delta}{4\delta^2 + [1 + (s/2)(1+4\delta^2)]^2}. \quad (2)$$

Here  $k_L$  is the wave vector,  $\delta = (\omega - \omega_o)/\Gamma$  is the normalized detuning of the laser frequency  $\omega$  relative to the atomic resonance  $\omega_o$ , and  $s$  is the saturation parameter given by  $s = s_0/(1+4\delta^2)$ , where  $s_0 = I/I_s$ . Figure 3 shows how the damping coefficient  $\alpha$  varies as the incident laser-beam intensity is changed, for a fixed detuning of  $-2.5\Gamma$ , at various radial distances from the axicon mirror axis. One can find that near a laser intensity of  $0.5 \text{ mW/cm}^2$ , the damping coefficients at several  $r$  positions are all above  $0.07\hbar k^2$ . For different values of the intensity, on the other hand,  $\alpha$  is very small at some values of  $r$ . One may think qualitatively that, as the damping coefficient becomes larger, more atoms can

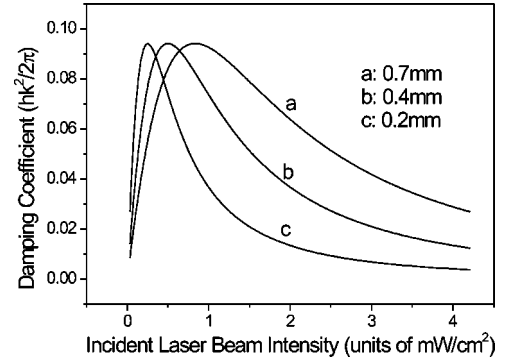


FIG. 3. The damping coefficient  $\alpha$  that varies with the incident laser-beam intensity as well as with the radial distance from the axicon mirror axis.

be extracted from the apex hole. Because  $\alpha$  is dependent on the radial position, however, one needs a careful Monte Carlo simulation in order to understand the results quantitatively.

We have performed a simple semi-classical Monte Carlo simulation of a pulsed CAB, which takes into account the increase of the laser intensity near the mirror axis as follows: the saturation parameter is now modified as  $s' = Rs/(r + r_0)$  in Eq. (2), where  $R$  is the entrance radius of the axicon and  $r_0$  is taken as the radius of the focused spot in the transverse plane of the mirror (for an axicon having a perfect cylindrical symmetry and a smooth surface,  $r_0$  can be chosen to be zero). Although we have used  $r_0 = 0.1 \text{ mm}$  in our simulation, we find that the numerical results are not sensitive to different values of  $r_0$ . Note that in considering the MOT on the axis away from the axicon apex, we have neglected, for simplicity, the effect that the laser intensity in the transverse direction decreases as one approaches the apex on the axicon axis.

Numerical simulations using up to 1000 rubidium atoms were performed for different combinations of laser intensity and detuning. The initial positions and velocities of the cooled and trapped atoms are described by the Gaussian distribution under typical MOT conditions. The mean position of the trapped atoms before being pushed is 5 mm in the axial direction, as measured from the axicon apex. The standard deviation of the position coordinate is 0.3 mm in all directions. The mean velocity of atoms is assumed to be zero in all directions, but its deviations in the longitudinal and transverse directions are 0.2 and 0.4 m/s, respectively. Note that the simulation results are not so sensitive to these initial conditions. During the pushing period, atoms are accelerated along the extraction column by the radiation-pressure force, and are exerted by the transverse scattering force given by  $F_T = -\alpha v_r$ , where the damping coefficient  $\alpha$  is given in Eq. (2).

The longitudinal radiation-pressure force in the presence of the transverse beams is smaller than that without them, since atoms can absorb not only the longitudinal laser but also the transverse laser. An obvious way to consider the transverse laser photons is to include a saturation term associated with the total intensity resulting from the longitudinal and transverse beams. Under this assumption, the longitudi-

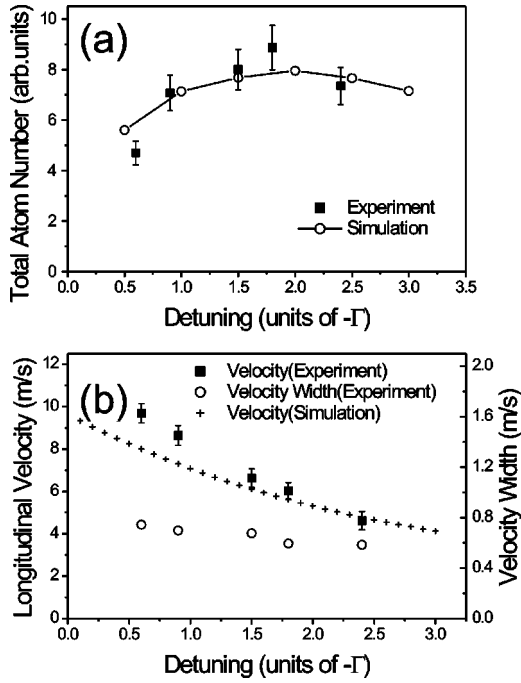


FIG. 4. (a) Experimental and simulational results for the total number of atoms in the CAB vs the pushing-beam detuning at a fixed intensity of  $I=0.64$  mW/cm<sup>2</sup>. (b) The mean value and the width of the atomic velocity distribution.

nal radiation-pressure force with the transverse laser beams present is given by

$$F_L = \hbar k_L \frac{\Gamma}{2} \frac{s_0}{1 + [1 + 2R/(r+r_0)]s_0 + [2(\delta - k_L v_z/\Gamma)]^2}. \quad (3)$$

We also consider diffusion effects due to spontaneous emission as follows. The total spontaneous decay rate is given by

$$R_t = \frac{\Gamma}{2} \frac{[1 + 2R/(r+r_0)]s_0}{1 + [1 + 2R/(r+r_0)]s_0 + 4\delta^2}, \quad (4)$$

which leads to the diffusion constant  $D_p = \hbar^2 k^2 R_t$ . In the simulation, the velocity of atoms is changed by a recoil velocity in a random direction in every time elapse of  $R_t^{-1}$ . As a result, the model we consider can be described by the simple differential equations given by

$$dv_r = (F_T/m)dt, \quad dv_z = (F_L/m)dt, \quad (5)$$

$$dr = v_r dt, \quad dz = v_z dt. \quad (6)$$

As one can observe in Figs. 2 and 4, these simple numerical simulations give reasonable accounts for the experimental results.

We have measured the mean velocity and the velocity spread of the CAB with respect to the intensity of the laser light [Fig. 2(b)]. As the intensity increases, the mean value and width of the CAB velocity distribution are increased together, whereas the fractional velocity spread remains almost unchanged ( $\Delta v/v \approx 0.12$ ). As can be seen, the experimental results are in good agreement with the simulational ones. Note that numerical calculation of the damping coefficient in Eq. (2) also exhibits behaviors versus the beam intensity similar to those shown in Fig. 2(a). We also have studied the change of the number of atoms in the CAB with respect to the laser detuning near the transition frequency [Fig. 4(a)], where the laser intensity is fixed at  $0.64$  mW/cm<sup>2</sup>. We observe that the experimental data are in good agreement with the simulation results. In particular, the maximum CAB flux is obtained at an optimum detuning of  $-1.7\Gamma$ , which is consistent with the experimental results of the thermal atomic beam collimated by a similar axicon [17]. We have also measured the atomic velocity and its spread versus the laser detuning, as shown in Fig. 4(b). We observe that as the detuning is increased, the mean value and width of the CAB velocity are decreased monotonically, whereas the fractional width ( $\Delta v/v$ ) shows no significant changes.

Finally, we have measured the divergence of our CAB from its spatial profile, which is obtained by detecting the absorption of the focused probe laser scanned across the CAB in the detection region. The divergence angle of the atomic beam is estimated as about  $150$  mrad, and the corresponding transverse temperature is  $380$   $\mu$ K. This is larger than the  $30$ -mrad divergence in the experiment by Lu *et al.* [7], and we conjecture that the difference may arise from the very low longitudinal velocity as well as the relatively large geometric solid angle in our CAB system (i.e., the shorter distance between the MOT and the axicon apex, and the hole diameter larger than the MOT size). Note that the atomic beam divergence may be reduced by employing two-dimensional magneto-optical cooling in the downstream of the axicon, as well as by making the hole size smaller.

In conclusion, due to its simplicity and convenience, optical generation of the CAB realized in the axicon funnel can be very useful in transporting the precooled atoms for atom optics experiments such as atom lithography, atom interferometer, and low-temperature atomic collision. In particular, the CAB in the conical or pyramidal funnel can be easily employed for loading the high-vacuum MOT's [8,9] or micro-atom-optical elements on a surface [13]. By using a larger axicon mirror with a smaller hole, and also using a more intense laser, one can produce a bright, continuous, slow CAB [14], which may be suitable, for example, for a simple, inexpensive, and even portable continuous CAB source for an improved atomic clock [18].

W.J. is grateful to Professor H. Ito for providing an axicon mirror. This work was supported by the Creative Research Initiatives of the Korean Ministry of Science and Technology.

- [1] See, for example, C.S. Adams, M. Sigel, and J. Mlynek, Phys. Rep. **240**, 143 (1994).
- [2] M.H. Anderson, J.R. Ensher, M.R. Matthews, C.E. Wieman, and E.A. Cornell, Science **269**, 198 (1995); K.B. Davis, M.-O. Mewes, M.R. Andrews, N.J. van Druten, D.S. Durfee, D.M. Kurn, and W. Ketterle, Phys. Rev. Lett. **75**, 3969 (1995).
- [3] W.D. Phillips and H. Metcalf, Phys. Rev. Lett. **48**, 596 (1982); T.E. Barrett, S.W. Dapore-Schwartz, M.D. Ray, and G.P. Lafaytis, *ibid.* **67**, 3483 (1991).
- [4] W. Ertmer, R. Blatt, J.L. Hall, and M. Zhu, Phys. Rev. Lett. **54**, 996 (1985).
- [5] M. Zhu, C.W. Oates, and J.L. Hall, Phys. Rev. Lett. **67**, 46 (1991).
- [6] W. Ketterle, A. Martin, M.A. Joffe, and D.E. Pritchard, Phys. Rev. Lett. **69**, 2483 (1992).
- [7] Z.T. Lu, K.L. Corwin, M.J. Renn, M.H. Anderson, E.A. Cornell, and C.E. Wieman, Phys. Rev. Lett. **77**, 3331 (1996).
- [8] R.S. Williamson III, P.A. Voytas, R.T. Newell, and T. Walker, Opt. Express **3**, 111 (1998).
- [9] J.J. Arlt, O. Marago, S. Webster, S. Hopkins, and C.J. Foot, Opt. Commun. **157**, 303 (1998).
- [10] K.I. Lee, J.A. Kim, H.R. Noh, and W. Jhe, Opt. Lett. **21**, 1117 (1996).
- [11] K.I. Lee, J.A. Kim, H.R. Noh, and W. Jhe, Proc. SPIE **2995**, 279 (1997); K.I. Lee, K.H. Kim, J.A. Kim, H.R. Noh, M. Ohtsu, and W. Jhe, J. Korean Phys. Soc. **33**, 365 (1998).
- [12] J.A. Kim, K.I. Lee, H.R. Noh, W. Jhe, and M. Ohtsu, Opt. Lett. **22**, 117 (1997).
- [13] J. Reichel, W. Hansel, and T.W. Hansch, Phys. Rev. Lett. **83**, 3398 (1999); R. Folman, P. Kruger, D. Cassettari, B. Hessmo, T. Maier, and J. Schmiedmayer, *ibid.* **84**, 4749 (2000).
- [14] D. Whitaker, S. Muniz, W. Jhe, and E. A. Cornell (unpublished).
- [15] Y.T. Chough and W. Jhe, J. Phys. Soc. Jpn. **69**, 1366 (2000).
- [16] J. Dalibard, S. Reynaud, and C. Cohen-Tannoudji, J. Phys. B **17**, 4577 (1984).
- [17] V.I. Balykin and A.I. Sidorov, Appl. Phys. B: Photophys. Laser Chem. **42**, 51 (1987).
- [18] W.F. Buell, Bull. Am. Phys. Soc. **44**, 726 (1999).